J Therm Anal Calorim (2010) 99:803–809
DOI 10.1007/s10973-009-0667-2

A thermal study approach to roman age wall painting mortars

A. Duran · L. A. Perez-Maqueda · J. Poyato · J. L. Perez-Rodriguez

MEDICTA2009 Special Issue

Abstract Roman ancient mortars have been widely studied, in connection with both diagnosis and application required for restoring. Thermoanalytical experiments performed on mortars from Pompeii and Herculaneum provided a very good understanding of the technology employed. The mortars from Pompeii were obtained by the proper mixing of lime and marble grains while mortars of Herculaneum by lime and silicates compounds. The position of the endothermic peak of calcite decomposition showed important variations in the different samples studied, which was assigned to the different crystallinity and particle sizes. Experiments under CO_2 flow confirmed the presence of magnesium calcium carbonates.

Keywords Historic mortars · Lime · Marble · TG–DTG–DTA · Carbonates decomposition · CO_2 flow

Introduction

Mortar is a composite material employed to assemble bricks or stone or as a finishing layer. The characterisation of ancient mortars provides useful information about how the complex architecture structures were built [1–5]. Lime was used in the antiquity as non-hydraulic cement mixed with pozzolane, specially to build duct drains, cistern and swimming pools [6, 7]. The hydraulic compounds are obtained from the reactions of $Ca(OH)_2$ with natural pozzolanes or artificial ones (such as ground fired bricks and tiles or ceramic shreds). The presence of aluminium and iron oxides together with the lime binder contributes to the mortar hydraulic character [8–11].

The function of natural or artificial pozzolanes, sand or marble grains (also frequently used) are to improve the mechanical properties of the resulting material and to reduce, as much as possible, the shrinkage occurring during the hardening. The binder, usually lime or hydraulic lime, is responsible for the hardening process [12].

Recently, raw material compositions, as well as the physical, mineralogical and microstructural characteristics of mortar samples from some historic buildings were determined to understand their technology and to produce compatible repair mortars with the existing ones in masonry structures [8, 13–15]. Literature reports [1, 4, 5, 8, 12] allow to group ancient mortars in two main categories: lime and hydraulic ones. In the first case, the hardening process arises from carbonation of dry or wet lime [16].

Wall painting may be defined as any painted design or composition applied directly to the surface of a building. Ranging from simple decorative patterns to more complex figurative or even narrative schemes, wall paintings form integral part of the monuments [13, 17–19]. The art of fresco in wall paintings was described by Vitruvius and Pliny the Elder [20, 21]. The wall is coated with a fresh mortar of lime and sand mixed with powdered marble. Coloured pigments are applied whilst the wall is still damp.

DTA/TG/DTG thermoanalytical investigations and X-ray diffractometry analyses allow the characterisation of the binding mortar materials, by specifying their main mineralogical components, as shown in other studies on

A. Duran (✉) · L. A. Perez-Maqueda · J. Poyato · J. L. Perez-Rodriguez
Materials Science Institute of Seville (CSIC-Seville University), Avda. Americo Vespucio, s/n, 41092 Seville, Spain
e-mail: adrian@icmse.csic.es

A. Duran
Centre de Recherche et de Restauration des Musées de France, CNRS-C2RMF UMR 171, 14 quai François Mitterrand, Palais du Louvre, 75001 Paris, France

ancient mortars [22–24]. References cited in literature indicate that DTA, along with TG, X-ray diffraction techniques, electron microscopy and high-temperature microscopy, are indispensable for the identification of mortars and for the determination of the degree of hydration and carbonation of limes in mortars. Furthermore, the recarbonation properties of limestones can be systematically and dependably studied using controlled atmosphere techniques [9].

Carbonates show distinctive endothermic peaks: at around 840 °C (calcite) and doublets at around 780 and at 860 °C (dolomite), whose position may vary depending on grain size, atmosphere and other concomitant factors. They are due to the escape of CO_2 during the breakdown of their structure. DTA is also capable of differentiating high-calcium limestones, dolomites and intermediate materials such as dolomitized limestones [9, 25–28].

The aim of this study implies the characterisation of mortars from Pompeii and Herculaneum, on which wall paintings 'on fresco' of the highest pictorial quality were found. Carbonate content variations and comparison between mortars collected in both archaeological sites are discussed.

Materials and methods

Mortars samples were collected during an archaeological rescue mission carried out by members of Fine Arts Faculty of Seville in Pompeii and Herculaneum cities.

Three mortars from the House of the Golden Bracelet in Pompeii (samples 15, 16 and 18 in the work) and two from Villa of Papyri in Herculaneum (samples 6 and 7 in the work), all of them samples dating back to 2nd B.C. in an excellent state of conservation and which have not been submitted to any restoration, were collected for this study. For the study, each mortar was divided by a scalpel (mechanical methods) in three parts, corresponding to the external, medium and internal layers, and studied separately. Cross-sections of the different samples, showing the different component layers and their thickness, and also the determination of pigments and binders using synchrotron radiation-high resolution X-ray powder diffraction, micro-XRD and conventional spectroscopy chromatography are shown in previous articles by the authors [18, 29].

Thermal Analysis was performed by means of a simultaneous TG/DTA, STD Q600 (TA Instruments). Measurements were conducted under flow of air or CO_2 and heated at a linear heating rate of 10 °C min^{-1}. The morphology of the different components of the mortars was observed in a HITACHI S-4800 Scanning Electron Microscope. The elemental analyses were performed using an X-ray energy dispersive spectrometer EDX Quantax 400 coupled to SEM. X-ray diffraction experiments were performed using a Siemens Kristalloflex D-5000 and analysis of XRD diagrams by the EVA package software. FTIR spectra were recorded by a Nicolet 510 spectrometer (source: Global, detector: DTGS) employed in transmission mode (using powder samples mixed with KBr) in the 4000–400 cm^{-1} range, with a resolution of 4 cm^{-1}. For each spectrum, at least 200 scans were accumulated and peak positions were determined using the Nicolet Omnic software, based on a polynomial least square method.

Results and discussion

SEM and EDX study

The results from these techniques showed important differences between the samples taken from the House of the Golden Bracelet in Pompeii (samples 15, 16 and 18) and those from Villa of Papyri in Herculaneum (samples 6 and 7). SEM images from the internal layers of samples 15, 16 and 18 showed large marble grains with irregular borders produced by grinding. Together with these grains appear small particles constituted by calcium carbonate produced by lime carbonation (Fig. 1a) according to EDX analysis, which only showed the presence of calcium (Fig. 1a). This calcium carbonate cements the grains of marble (primary calcite used as aggregate). Other compounds such as silicates were not found. The external and medium layers showed similar composition to the internals; however, mercury and sulphur were detected in the external layer of sample 16, and also small amounts of iron in 15 and 18, and copper in 18. Primary calcite inclusions are uncalcined calcium carbonate, which is a limestone containing coarse-grained calcite crystals. This material possibly has been ground and added to the slaked mixture (or it was not calcined properly in the first place). The addition of uncalcined calcium carbonate to plaster mixtures was known in later periods (Roman plaster) where marble dust, essentially uncalcined calcium carbonate, was recommended by Vitruvius to be added to plaster to give it an improved white shine and lustre [18, 20, 30].

The samples 6 and 7 showed different morphology to the previously studied samples. Marble grains did not appear being only present small particles attributed to carbonation of the original binder (lime putty) (Fig. 1b). The EDX analysis of the internal layers showed the presence of calcium and small proportion of magnesium (Fig. 1b); in addition, silicium, aluminium, potassium and iron were detected, possibly from silicate compounds that could be attributed to hydraulic components. In the external layers only calcium was found.

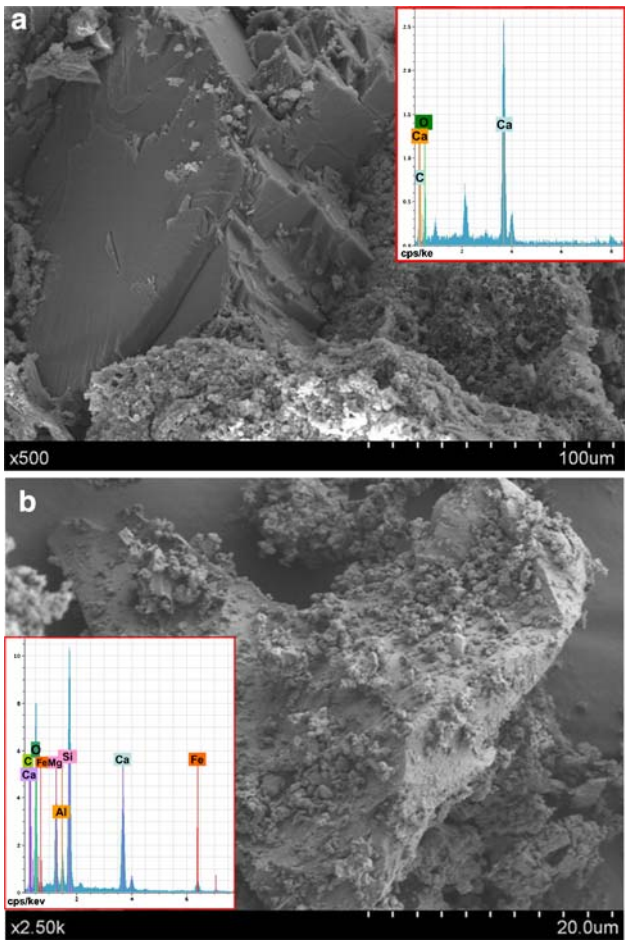

Fig. 1 SEM images and EDX analysis of internal layers of: **a** Mortar 18 from Pompeii; **b** Mortar 6 from Herculaneum

FT-IR study

FT-IR spectra of the external, medium and internal layers of sample 6 are shown in Fig. 2a. Similar IR absorption bands at 1790–1797, 1425–1428, 874 and 710–712 cm^{-1} assigned to calcium carbonate [31, 32] were detected in the three layers of this mortar. In the internal layer, a band at 1018 cm^{-1} assigned to silicate [31] has been found. These data showed that the internal layer was carried out using a siliceous mineral (evidence of the presence of hydraulic components) and a binder (lime). Similar results were observed in the three layers of sample 7, with calcium carbonate and silicates in the internal one. Both types of compounds were also present in the medium layer of this sample, but with lower proportion of silicate compounds.

The different layers of the three mortars from The House of the Golden Bracelet in Pompeii (samples 15, 16 and 18) showed IR spectra with similar absorption bands which were assigned to calcite. No other compounds were detected by FT-IR spectroscopy (Fig. 2b).

XRD study

This technique confirmed the differences in composition between the mortars collected from the House of the Golden Bracelet in Pompeii and those from Villa of Papyri in Herculaneum.

The X-ray diffraction diagrams of internal layer of sample 6 showed diffraction peaks at $d = 3.03$, 2.28 and 2.10 Å attributed to calcite ($CaCO_3$). In addition, other peaks were detected at 3.19 and 3.18 Å, which were assigned to anorthite ($CaAl_2Si_2O_8$) (Fig. 3a). This experiment confirmed that this layer was made using a siliceous material and lime as binder. However, the medium and external layers were constituted only by calcite. Similar results were found previously by SEM and FT-IR studies. In sample 7, the internal and medium layers showed diffractions attributed to calcite and anorthite by XRD. In the external, only calcite was found (Fig. 3b).

Only calcite appeared in the internal and medium layers of samples 15, 16 and 18. In the external layers, calcite was accompanied by other phases attributed to the coloured pigments applied to the wall, as was described in previous articles of the authors [18, 29]. In sample 15, haematite ($d = 2.70$, 2.52 Å) (Fe_2O_3) and aragonite ($d = 3.39$, 3.27 Å) ($CaCO_3$) were found. Haematite is a red pigment frequently used and aragonite has been applied as a white pigment because of its higher hiding powder in comparison with calcite [33]. In sample 18, cuprorivaite ($d = 3.28$, 3.78 Å) ($CaCuSi_4O_{10}$) was detected together with haematite and aragonite (Fig. 3c). Cuprorivaite is the crystalline

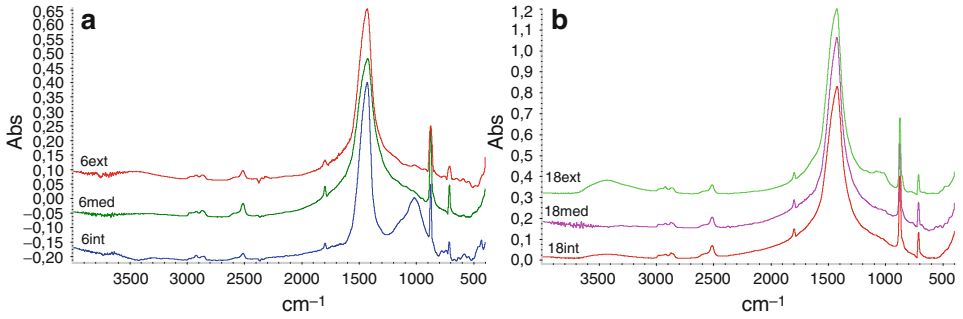

Fig. 2 FT-IR spectra performed on all the layers of: **a** Mortar 6; **b** Mortar 18

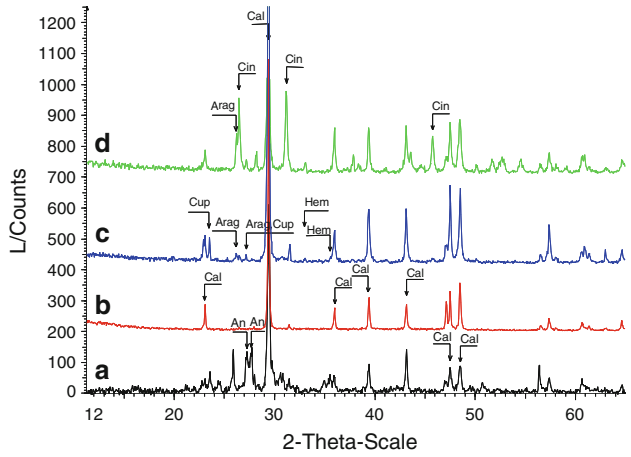

Fig. 3 XRD diagrams collected on: **a** Internal layer of mortar 6; **b** External layer of mortar 7; **c** External layer of mortar 18; **d** External layer of mortar 16. (*Cal* calcite; *An* anorthite; *Ar* aragonite; *Cup* cuprorivaite; *Hem* hematite; *Cin* cinnabar)

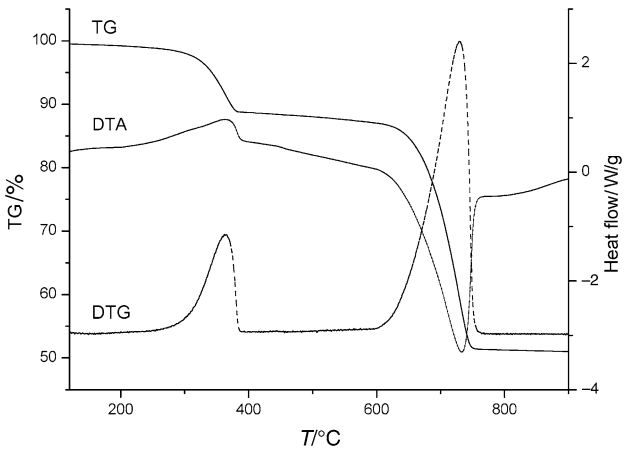

Fig. 4 TG/DTA/DTG curves of the external layer of mortar 16

phase corresponding to the pigment Egyptian blue, also called Pompeian blue, which is an artificial pigment, prepared by heating of a mixture that contains silica (SiO_2), a compound of copper (possibly malachite), calcium carbonate and sodium carbonate [18, 34], although this is also a rare mineral that it is present as a natural component in the lava of Vesuvio. In the external layer of sample 16, vermilion (HgS), a red colour pigment, was found ($d = 3.36$, 2.86, 1.98 Å) (Fig. 3d), and also calcite and aragonite. Vermilion originally derived from the powdered mineral cinnabar. The cinnabar mines used by the Romans were Spanish, as Theophastur asserted 200 years before Vitruvius [35].

Thermal study

The mass loss between 620–640 °C and 780 °C of TG curves was used to calculate the carbonate content of the studied samples (Table 1). The internal layer of sample 6 showed the presence of 34% of carbonate accompanied of 66% of siliceous material. However, in the medium and external layers only carbonate was present (100%). In the internal layer of sample 7, the carbonate content was 67%, higher than in the former sample, being also present about 33% of silicates material. In the medium layer, the percentage of silicates material was lower, about 11%.

In the other studied samples, carbonate was practically the only present compound, except in the external layer of sample 16 where carbonate percentage only reached a value of 78.4%. The TG curve of this external layer, where the pigment layer is included (10–20 μm), showed a mass loss (∼10%) between 310 and 375 °C corresponding to an exothermic effect in the DTA curve (Fig. 4), which was also present in the thermal study carried out in CO_2 atmosphere. This effect has been attributed to the process of dissociation–sublimation of HgS [36]. Cinnabar was previously detected by XRD.

In all the samples studied in this work, except in the external layer of sample 16, a continuous mass loss of about 1.2–2.5% has been found between room temperature and 620 °C. For mortars, in the temperature range from 30 to 120 °C the mass loss is due to adsorbed water, from 120 to 200 °C the mass loss of water from hydrated salts occurs, between 200 and 600 °C the mass loss is due to structurally bound water from the hydraulic compounds and, finally, the loss of CO_2 as a consequence of the decomposition of calcium carbonate ($CaCO_3$) takes place at temperature range between 650 and 850 °C [13, 25]. In this form, the small amount of mass loss between room temperature and 620 °C of the samples studied in this work showed the small content of adsorbed water, hydrated salts and bound water; only in the internal layer of sample 6 was a little higher, 2.5%, probably due to the presence of siliceous material, hydraulic components, in this mortar.

The DTG curves corresponding to carbonate decomposition of the internal layers of mortars from Villa of Papyri

Table 1 Carbonate content of the samples calculated from the mass loss between 620–640 °C and 780 °C

Sample	6i	6m	6e	7i	7m	7e	15i	15m	15e	16i	16m	16e	18i	18m	18e
% Carbonate content	34	100	100	67	89	95	99	100	100	97	100	78	97	100	100

i internal; *m* medium; *e* external

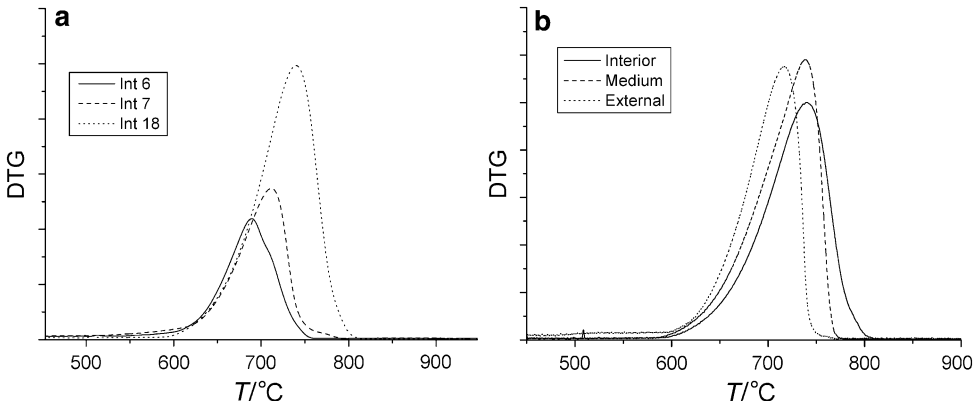

Fig. 5 DTG curves showing the carbonate decomposition peaks of: **a** Internal layers of mortars 6, 7 and 18; **b** Internal, medium and external layers of mortar 18

in Herculaneum (samples 6 and 7) and from the House of the Golden Bracelet in Pompeii (sample 18) are shown in Fig. 5a. Differences in the maximum of DTG peaks are shown: in sample 6 the maximum appeared at 695 °C with a shoulder at 712 °C, at 720 °C in the sample 7, and the highest value appeared in sample 18 at 745 °C. The decomposition of calcite materials in fact may vary in a large temperature range as a function of the history of the material (it may contain recarbonated lime), experimental conditions, degree of fragmentation and crystallinity of the material. Monocrystalline calcite undergoes complete decarbonation at temperatures higher than 750 °C while polycrystalline materials, such as limestone or chalk, in some cases, start to decompose at temperatures lower than 650 °C [9, 12, 37]. The peak for a calcium carbonate sample prepared by recarbonation of calcium hydroxide occurs at a lower temperature than that for the original carbonate from which the hydroxide was prepared. This fact is attributed to the finer particle size of the secondary carbonate [26]. The highest value of the DTG peak that appeared in the internal layer of sample 18 should be attributed to the presence of monocrystalline calcite, whereas the presence of polycrystalline calcite in the internal layer of sample 6 was responsible for the lowest value (Fig. 5a).

A decrease in the temperature maximum of DTG peaks appeared comparing the internal, medium and external layers of samples 15, 16 and 18 (Fig. 5b). The original sample was only disaggregated before carrying out the thermal study not to decrease the particles' size by grinding. This fact should be attributed to a decrease of particle size of material and crystallinity of material [38–40], being the finest particles present in the external layers.

Two peaks appear in dolomite decomposition curves. The first peak is due to the decomposition of the carbonate ions associated with magnesium and the second peak to the decomposition of those associated with calcium. The low substitution of calcium by magnesium in calcite structure is difficult to characterise by thermal analysis. In this case, the two possible peaks are more clearly resolved in a carbon dioxide atmosphere. The use of a carbon dioxide atmosphere during the heating raises the calcite peak temperature and considerable sharpens [9, 25–28].

The thermal study performed on all the layers of mortars 15,16 and 18 and on the external layers of 6 and 7, heating in air, only showed a shift at lower temperature in the mass loss than under flow of CO_2 (Fig. 6a). The TG curve of internal layer of mortar 6, carried out in air atmosphere showed only a mass loss between 625 and 740 °C. However, the heating in CO_2 atmosphere shifted the mass loss

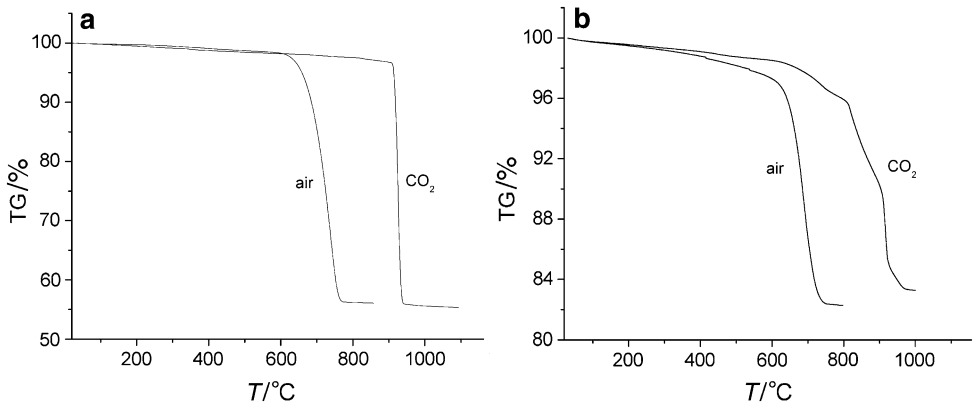

Fig. 6 TG curves under air and CO_2 flows of: **a** External layer of mortar 6; **b** Internal layer of mortar 6

peak at higher temperature and showed a splitting of the curve in comparison with the heating in air atmosphere (Fig. 6b). This fact was attributed to the decomposition of carbonates in several steps, magnesium being present in the calcite structure. The presence of magnesium together with calcium was confirmed by EDX analysis as was previously described in this article.

Conclusions

The mortars from Villa of Papyri in Herculaneum were obtained by the proper mixing of a binder, lime, with a material as silicate (anorthite). The mortars from the House of the Golden Bracelet in Pompeii were obtained by the mixing of a binder like lime, however, as aggregate material was used marble grains prepared by grinding.

The thermal analysis showed differences in the temperature of the carbonate thermal decomposition. The temperature was higher in mortars that contained marble grains than carbonate produced by lime carbonation. This fact should be attributed to the higher monocrystallinity of the marble particles. The use of smaller grains and more content of lime in the external layers of samples from the House of the Golden Bracelet in Pompeii produced a shift at lower temperature of the carbonate thermal decomposition.

The thermal study on the internal layer of mortars from Herculaneum, conducted under flow of CO_2, showed a splitting of the TG curve attributed to carbonate thermal decomposition, confirming the presence of some magnesium in the lime used as binder in agreement with the results obtained by SEM–EDX.

The presence of cinnabar (HgS) used as pigment in the wall paintings on the external layers of the mortar (sample 15) was detected by DTA/TG study and also by XRD.

Acknowledgements The authors gratefully acknowledge Dr. E. Millan (Fine Arts Faculty of Seville), Dra. M.C. Jimenez and Dr. A. Justo (ICMSE staff) and C2RMF staff for their assistance, and the financial support from contract MEC/FULLBRIGHT-FECYT 2007 and project MAT2008-06619/MAT (MICINN).

References

1. Bakolas A, Biscontin G, Moropoulou A, Zendri E. Characterisation of structural Byzantine mortars by thermogravimetric analysis. Thermochim Acta. 1998;321:151–60.
2. Franzini M, Leoni L, Lezzerini M, Sartori F. The mortar of the leaning Tower of Pisa—the product of a medieval technique for preparing high-strength mortars. Eur J Miner. 2000;12(6):1151–63.
3. Moropoulou A, Bakolas A, Bisbikou K. Investigation of the technology of historic mortars. J Cult Herit. 2000;1(1):45–58.
4. Pires J, Cruz AJ. Techniques of thermal analysis applied to the study of cultural heritage. J Therm Anal Calorim. 2007;87(2):411–5.
5. Rizzo G, Megna B. Characterization of hydraulic mortars by means of simultaneous thermal analysis. J Therm Anal Calorim. 2008;92(1):173–8.
6. Harries KA. Concrete construction in early Rome. Concr Int. 1995;1:58–62.
7. Marusin SL. Ancient concrete structures. Concr Int. 1996;1:56–8.
8. Bakolas A, Biscontin G, Contardi V, Franceschi E, Moropoulou A, Palazzi D, et al. Thermoanalytical research on traditional mortars in Venice. Thermochim Acta. 1995;269/270:817–28.
9. Moropoulou A, Bakolas A, Bisbikou K. Characterization of ancient Byzantine and later historic mortars by thermal and X-ray diffraction techniques. Thermochim. Acta. 1995;269/270:779–95.
10. Alvarez JI, Navarro I, Garcia-Casado PJ. Thermal, mineralogical and chemicals studies of the mortars used in the cathedral of Pamplona (Spain). Thermochim Acta. 2000;365:177–87.
11. Maravelaki-Kalaitzaki P, Moropoulou A, Bakolas A. Physico-chemical study of Cretan ancient mortars. Cem Concr Res. 2003;33:651–61.
12. Cardiano P, Sergi S, De Stefano C, Ioppolo S, Piraino P. Investigations on ancient mortars from the Basilian monastery of Fragala. J Therm Anal Calorim. 2008;91(2):477–85.
13. Duran A, Robador MD, de Jimenez Haro MC, Ramirez-Valle V. Study by thermal analysis of mortars belonging to wall paintings corresponding to some historic buildings of Sevillian art. J Therm Anal Calorim. 2008;92(1):353–9.
14. Moropoulou A, Cakmar S, Biscontin G, Bakolas A, Zendri E. Advanced Byzantine cement based composites resisting earthquake stresses: the crushed brick/lime mortars of Justinian's Hagia Sophia. Constr Build Mater. 2002;16(8):543–52.
15. Rossi-Doria PR. Mortars for restoration: basic requirements and quality control. Mater Struct. 1986;19(114):445–8.
16. Stepkowska ET, Aviles MA, Blanes JM, Perez-Rodriguez JL. Gradual transformation of $Ca(OH)_2$ into $CaCO_3$ on cement. J Therm Anal Calorim. 2007;87(1):189–98.
17. Anastasiou M, Hasapis T, Zorba T, Plavidou E, Chrissafis K, Paraskevopoulos K. TG-DTA and FTIR analyses of plasters from byzantine monuments in Balkan region. J Therm Anal Calorim. 2006;84(1):27–32.
18. Duran A, Jimenez de Haro MC, Perez-Rodriguez JL, Franquelo ML, Herrera LK, Justo A. Determination of pigments and binders in Pompeian wall paintings using synchrotron radiation-high resolution X-ray powder diffraction and conventional spectroscopy-chromatography. Archaeometry 2009. doi 10.1111/j.1475-4754.2009.00478.x.
19. Duran-Benito A, Herrera-Quintero LK, Robador-Gonzalez MD, Perez-Rodriguez JL. Color study of Mudejar paintings of the pond found in the palace of Reales Alcazares. Color Res Appl. 2007;32(6):489–95.
20. Vitruvius. In: M.H. Morgan, editor. De Architectura Libri decem, II (Materials) and VII (Finishes and colours). Whitefish: Kessinger Publishing; 2005. p. 493.
21. Pliny the Elder, Natural History. Paris: Societe d'Editions Les Belles letters (ed); 1985. p. 317.
22. Bruno P, Calabrese D, Di Pierro M, Genga A, Laganara C, Manigrassi D, et al. Thermical-physical and mineralogical investigation of ancient mortars from the archaeological site of Monte-Sannace. Thermochim Acta. 2004;418:131–41.
23. Riccardi MP, Duminuco P, Tomasi C, Ferloni P. Thermal, microscopic and X-ray diffraction studies on some ancient mortars. Thermochim Acta. 1998;321:207–14.
24. Biscontin G, Pellizon M, Zendri E. Characterization of binders employed in the manufacture of Venetian historical mortars. J Cult Herit. 2002;3(1):31–7.
25. Genestar C, Pons C, Más A. Analytical characterisation of ancient mortars from the archaeological Roman city of Pollentia (Balearic Islands, Spain). Anal Chim Acta. 2006;557(1–2):373–9.

26. Webb TL, Krüger JE. Carbonates. In: Mackenzie RC, editor. Differential thermal analysis. London: Academic Press; 1970. p. 303–41.
27. Vágvölgyi V, Frost RL, Hales M, Locke A, Kristof J, Horváth E. Controlled rate thermal analysis of hydromagnesite. J Therm Anal Calorim. 2008;92(3):893–7.
28. Beck CW. Differential thermal analysis curves of carbonate minerals. Am Miner. 1950;35:985–1013.
29. Duran A, Castaing J, Walter P. X-ray diffraction studies of Pompeian wall paintings using synchrotron radiation and dedicated laboratory systems. Appl Phys A. (Article accepted).
30. Brysbaert A. Painted plaster from Bronze Age Thebes, Boeotia (Greece): a technological study. J Archaeol Sci. 2008;35:2761–9.
31. Farmer VC. Infrared spectra of minerals. In: Farmer VC, editor. Mineralogical Society Monograph 4. London: Mineralogical Society; 1974. p. 399.
32. Ji J, Ge Y, Balsam W, Damuth JE, Chen J. Rapid identification of dolomite using a Fourier Transform Infrared Spectrophotometer (FTIR): a fast method for identifying Heinrich events in IODP Site U1308. Mar Geol. 2009;258(1–4):60–8.
33. Baraldi P, Baraldi C, Curina R, Tassi L, Zannini P. A micro-Raman archaemetric apporach to Roman wall paintings. Vib Spectrosc. 2007;43(2):420–6.
34. Laurie AP, McLintock WF, Miles FD. Egyptian blue. In: Proceedings of the Royal Society of London, Series A. 1914, p. 418–429.
35. Mazzochin GA, Baraldi P, Barbante C. Isotopic analysis of lead present in the cinnabar of Roman wall paintings from the X Regio (Venetia et Histria). Talanta. 2008;74(2):690–3.
36. Baláz P, Post E, Bastl Z. Thermoanalytical study of mechanically activated cinnabar. Thermochim Acta. 1992;200:371–7.
37. Shoval S, Gaft M, Beck P, Kirsh Y. Thermal behaviour of limestone and monocrystalline calcite tempers during firing and their use in ancient vessels. J Therm Anal Calorim. 1993;40(1):263–73.
38. Perez-Maqueda LA, Perez-Rodriguez JL, Scheiffele GW, Justo A, Sanchez-Soto PJ. Thermal analysis of ground kaolinite and pyrophyllite. J Therm Anal. 1993;39(8–9):1055–67.
39. Perez-Maqueda LA, Blanes JM, Pascual J, Perez-Rodriguez JL. The influence of sonication on the thermal behavior of muscovite and biotite. J Europ Ceram Soc. 2004;24(9):2793–801.
40. Perez-Rodriguez JL, Pascual J, Franco F, de Haro MCJ, Duran A, del Valle VR, Perez-Maqueda LA. The influence of ultrasound on the thermal behaviour of clay minerals. J Europ Ceram Soc. 2006;26(4–5):747–53.